# Vector Magnetic Properties Measurement of Silicon Steel Under Biased Magnetic Excitation Along Laminated Direction

Changgeng Zhang[1,2], Xinxiao Yan[1,2], Yongjian Li[1,2], and Qingxin Yang[1,2,3]

[1]State Key Laboratory of EERI, School of Electrical Engineering, Hebei University of Technology, Tianjin 300130, China
[2]Hebei Province Key Laboratory of EFEAR, Hebei University of Technology, Tianjin 300130, China
[3]Tianjin Key Laboratory of AEEET, Tianjin Polytechnic University, Tianjin 300387, China

**Rotational magnetic flux in the plane of steel laminations causes core losses which far exceed than alternating magnetic flux. Traditional testing methods such as Epstein frame detected only in one direction may lead to inaccurate predictions of core losses. This paper developed a 3-D magnetic properties testing device to measure the magnetic properties of high grain-oriented silicon steel. By using the automatic control system and novel surface *B–H* sensing coils, the dynamic magnetic hysteresis properties of the silicon steel are accurately measured with a static magnetic field along the laminated direction of the specimen. Finally, an ellipsoid magnetic anisotropy model is established which parameters can be identified by the magnetic measurement results with biased magnetic field.**

***Index Terms*—3-D magnetic property, biased magnetic excitation, rotational core losses, silicon steel sheet.**

## I. Introduction

THE complex nonlinear magnetic properties of laminated silicon steel are critical factors in designing and optimizing of electrical equipment such as power transformer and electrical machine [1]. The rotational core losses in the stator of electrical machines and T-joints of three-phase transformers may be up to more than 50% of total core losses [2]. However, traditional testing methods such as Epstein frame and single sheet tester can only detect 1-D magnetic property, which may lead to inaccurate predictions of iron loss [3], [4]. Besides, in the electromagnetic simulation, the three independent magnetization curves in three directions are commonly adopted as the model of soft magnetic material, which would cause significant numerical errors, especially for magnetic anisotropy material. Besides, for grain-oriented (GO) silicon steel, rotational magnetic flux in the plane of steel laminations causes iron losses which far exceed than alternating magnetic flux [5], [6]. Therefore, 3-D coupling magnetic properties of the laminated silicon steel in the 3-D complex magnetization conditions should be taken into account [7].

A 3-D magnetic properties tester was designed to measure the non-GO silicon steel sheet 35ww270 and soft magnetic composite materials [8]. These magnetic hysteresis loops and the corresponding loss properties under alternating and 2-D rotational magnetization were measured and analyzed at 50 Hz. The automatic control system was developed to obtain the standard sinusoidal waveform and circular magnetic loci [9].

In this paper, the magnetization testing system has been improved to measure the 3-D magnetization loci under the dc-biased magnetic along the laminated direction in order to analyze the magnetic anisotropy properties of silicon steel. Then, the complex ac and dc hybrid magnetization model is developed, which combines the static magnetic field along the laminated direction with an arbitrary 2-D magnetic field in sheet plane. Relying on the measured 3-D magnetic properties data under dc-bias magnetic field, the 3-D magnetic anisotropy model is established and identified.

Manuscript received June 5, 2018; revised August 5, 2018 and August 30, 2018; accepted August 31, 2018. Date of publication September 26, 2018; date of current version January 18, 2019. Corresponding author: C. Zhang (e-mail: changgeng.zhang@hebut.edu.cn).
Digital Object Identifier 10.1109/TMAG.2018.2868883

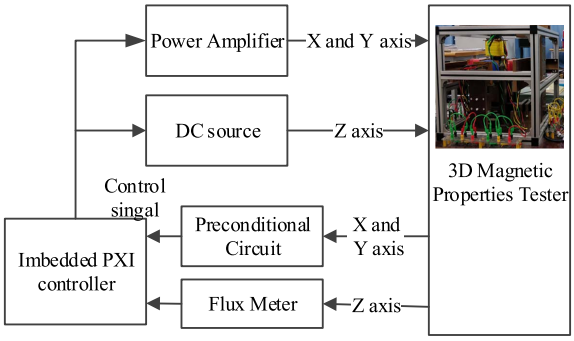



Fig. 1. Block diagram of 3-D magnetization testing system with dc excitation along the laminated direction.

## II. 3-D Magnetic Testing System

### A. Improved 3-D Testing System

Fig. 1 shows the improved 3-D magnetic testing system, which consists of 3-D magnetization properties tester, imbedded PCI extensions for instrumentation controller, flux meter, two channels of AC power amplifier, and one DC current source. The dc current source is used to excite the static magnetic field along the laminated direction inside the specimen, while the ac power amplifiers are used to excite arbitrary 2-D flux trajectory in the plane of silicon steel sheet. The static magnetic flux density can be integrated by the magnetic flux meter.

Compared with the 2-D magnetic testing system, the 3-D magnetization system has a higher exciting current and a larger core size with 0.7 m length side. The automatic feedback system operated in the LabVIEW environment can precisely generate the required excitation waveform.

Because the magnetic testing system is nonlinear, the digital feedback performed in LabVIEW for magnetic measurement

0018-9464 © 2018 IEEE. Personal use is permitted, but republication/redistribution requires IEEE permission.
See http://www.ieee.org/publications_standards/publications/rights/index.html for more information.

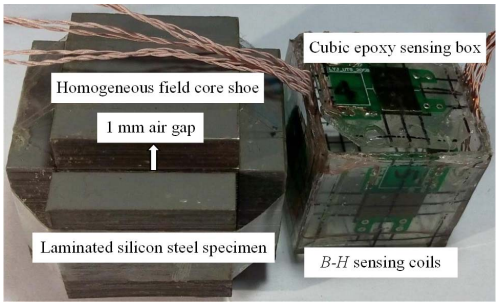



Fig. 2. Laminated silicon steel specimen (27zh95) and $B$–$H$ sensing coils.

has the advantage to fulfill complex scheme. The errors of averaged magnetic field strength between clockwise (CW) and counter-clockwise (CCW) rotation can be up to 1% without feedback control. Even if a slight difference between the two working conditions would cause significant errors. The three channels of excitation signal are controlled by the proportional–integral–derivative controller, in which the feedback is the electromotive force (EMF) of $B_{\mathbf{x}}$ and $B_{\mathbf{y}}$. The control algorithm can make sure the working condition of CW and CCW rotation remains the same, which can reduce error below 0.3%.

### B. 3-D Magnetic Property Sensing System

The 3-D magnetic property sensing system consists of 3-D magnetic sensing coil, signal preconditioning circuit with high resolution, and data acquisition hardware and software. The square $H$ and circular $B$ coil are combined together, which is embedded in the center of the epoxy resin frame [8]. The induction coils are closely attached to the surface of specimen to obtain the correct induction voltage values of the $B$ and $H$ sensing coils as illustrated in Fig. 2. Six homogeneous field core shoes with the same material and the laminated direction around the cubic specimen are designed to homogenize the magnetic field. There is 1 mm air gap between the specimen and the homogeneous field core shoe which is beneficial to decouple the magnetic flux from different excitation axes. The homogeneous field core shoes can be regarded as the extension of the specimen. As a result, the specimen and their homogeneous field core shoes merge into a larger specimen. Then, the internal cubic of the larger specimen has a much more homogeneous magnetic field.

According to the Faraday's law, $B$ and $H$ inside silicon steel can be calculated by measuring the corresponding EMF of the induction coil. Meanwhile, the static magnetic flux in $z$-axis can be measured by the flux meter using the numerical integration of the changing EMF during the transient change of excitation current.

## III. Experimental Measurement

Using the 3-D magnetic testing system, several typical magnetization models have been carried out to investigate dynamic magnetic properties of GO silicon steel.

### A. Rotating Magnetization Model

For a 2-D excitation model, a set of excitation signal is given in the $xoy$ plane to obtain circular or elliptical $B$ loci

$$\begin{aligned} u_x(t) &= \alpha U_m \sin(\omega t + \phi) \\ u_y(t) &= U_m \cos(\omega t + \phi) \end{aligned} \tag{1}$$

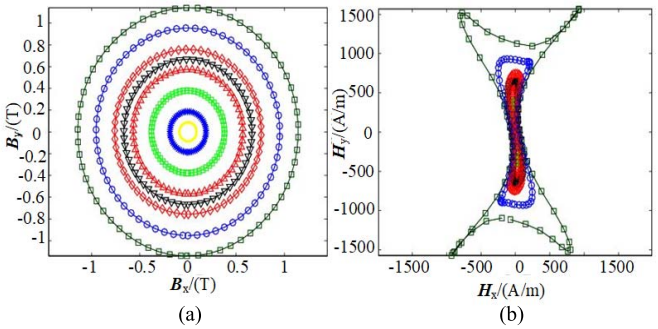



Fig. 3. Rotational magnetic properties of silicon steel 27zh95. (a) Circular $\boldsymbol{B}$ loci. (b) Corresponding $\boldsymbol{H}$ loci.

where $\omega$ is angular frequency and $\alpha$ is the axis rate of the ellipse.

Fig. 3 demonstrates the rotational magnetic properties in sheet plane when the specimen is magnetized with increasing $\boldsymbol{B}$ up to 1.2 T at 50 Hz. The control algorithm makes sure that the loci of $B$ are always circular. When, the magnetic flux density is less than 0.9 T, $\boldsymbol{H}$ loci first become shapes of saddle, then approximately evolve to shapes of rectangle with the increasing current. When, $B$ is larger than 0.9 T, the loci of $\boldsymbol{H}$ vector appear spikes at the direction about 55° with $x$-axis. Moreover, the $x$-intercepts of $\boldsymbol{H}$ loci are much smaller than those of $\boldsymbol{H}$ loci, which reflects that the transverse direction of silicon steel is more difficult to be magnetized.

### B. AC and DC Hybrid Magnetization Model

In order to analyze the influence of dc bias magnetic field along the laminated direction, an ac and dc hybrid magnetization model is established. The 3-D complex model can be described as the following:

$$\begin{cases} B_x = B_{\max} \sin(\omega t + \theta) \\ B_y = B_{\max} \sin(\omega t + \theta) \\ B_z = B_0 \end{cases} \tag{2}$$

where $B_{\max}$ is the amplitude of $\boldsymbol{B}$ and $B_z$ is controlled as a constant value $B_0$. The windings in $x$- or $y$-axis are excited by alternating sinusoidal current, while the windings in $z$-axis are excited by dc current ranging from 0 to 3 A. The alternating magnetization results are measured in the rolling direction ($x$-axis) and the transverse direction ($y$-axis) at the frequency of 50 Hz.

When, the alternating excitation model is applied in the laminated direction, there would be significant eddy current in the plane of silicon steel sheet because of skin effect of magnetic field. Moreover, eddy current is strongly dependent on the shape of silicon steel specimen. Then, $B$ along the laminated direction is far from uniform. Consequently, dc magnetic flux is still chosen as the excitation model along the laminated direction even if the dc-biased magnetic flux is rare in the electrical apparatus such as electrical motor and power transformer.

Fig. 4 illustrates a group of $B$–$H$ hysteresis loops under different sinusoidal excitations. The result demonstrates that the silicon steel is much easier to be magnetized in the rolling direction than that in the transverse direction. Meanwhile, the saturation magnetic flux density in the transverse direction is much smaller than that in the rolling direction.

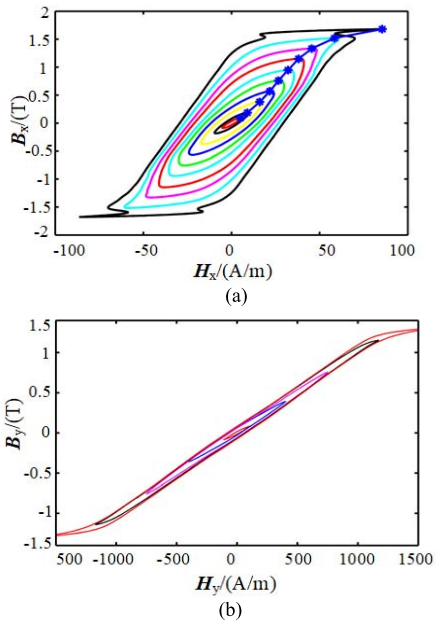



Fig. 4. Family of Hysteresis loops under alternating magnetization excitations. (a) $H_x$–$B_x$ loops in the rolling direction ($x$-axis). (b) $H_y$–$B_y$ loops in the transverse direction ($y$-axis).

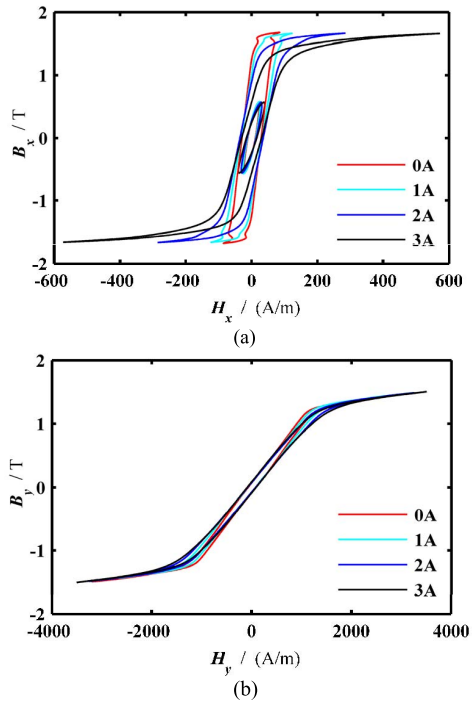



Fig. 5. Family of Hysteresis loops under ac and dc hybrid excitation model. (a) Hysteresis loops of $H_x$–$B_x$ under the static magnetic field in $z$-axis. (b) Hysteresis loops of $H_y$–$B_y$ under the static magnetic field in $z$-axis.

Fig. 5 illustrates a series of hysteresis loops in the rolling and the transverse directions under ac and dc hybrid excitation model with different amplitudes of ac and dc excitation current. It is concluded that the larger static magnetic field excited in the laminated direction of silicon steel, the more difficult the rolling and the transverse direction are magnetized.

Fig. 6 shows the magnetization curves under different dc-biased magnetic field along the laminated direction. The magnetization curves shift downwards with increasing the biased

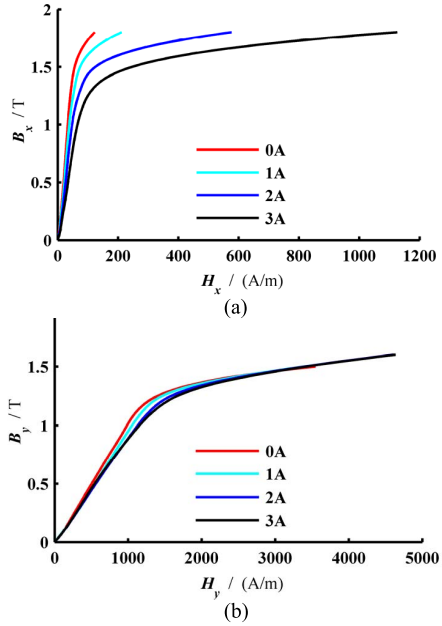



Fig. 6. Magnetization curves under different magnitudes of dc-biased magnetic field along the laminated direction. (a) Rolling direction. (b) Transverse direction.

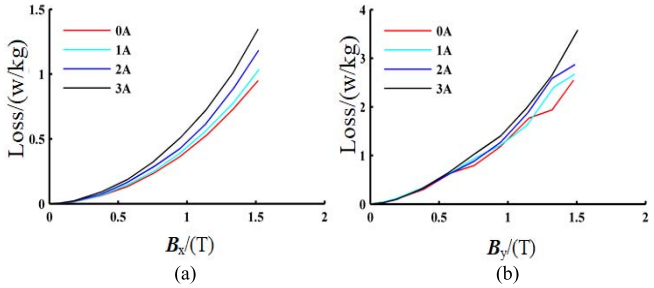



Fig. 7. Core losses under different dc-biased magnetic field along the laminated direction. (a) Rolling direction. (b) Transverse direction.

dc current. Since, the magnetic permeability in the rolling direction is much smaller than that in the transverse direction, the magnetic properties in the rolling direction is more sensitive than that in the transverse direction.

Fig. 7 demonstrates corresponding core losses of silicon steel 27zh95 under ac and dc hybrid excitation model. Compared with the results, the core losses in the rolling direction are smaller than those in the transverse direction. Besides, the core losses in both the rolling and the transverse direction are increasing when the static magnetic field rises in the laminated direction.

## IV. Modeling of Magnetic Properties Under DC-Biased

Various models of magnetic anisotropy are based on the experimentally determined family of magnetization curves. By observing the magnetic anisotropy in 3-D space, the relationship among $B_x$, $B_y$, and $B_z$ within a specific range can be expressed by an ellipsoid model

$$\frac{B_x^2}{\mu_x^2}+\frac{B_y^2}{\mu_y^2}+\frac{B_z^2}{\mu_z^2}=H_x^2+H_y^2+H_z^2 \tag{3}$$

where $\mu_x$, $\mu_y$, and $\mu_z$ are the magnetic permeability of the silicon steel, respectively. The magnetic field strength $H$ is

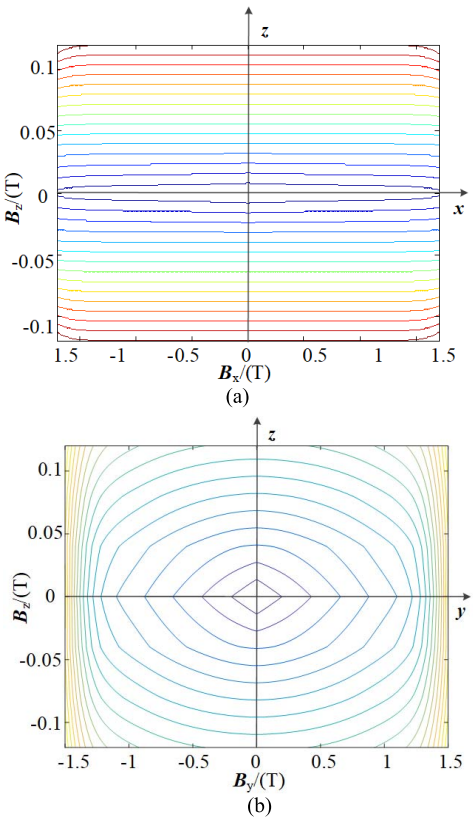



Fig. 8. Magnetic energy contour of high GO silicon steel under ac and dc hybrid magnetization model. (a) Energy ($H^2$) contour in $xoz$ plane. (b) Energy ($H^2$) contour in $yoz$ plane.

defined as vector summation of the magnetic field strength on the $x$-, $y$-, and $z$-axis directions.

In the traditional magnetic properties model $H$ can be calculated directly by the 1-D magnetization curve

$$H_i = \frac{B_i}{\mu_i}, \quad i = x, y, z. \tag{4}$$

In the proposed model, $\mu_x$, $\mu_y$, and $\mu_z$ are functions of 3-D space. The loci of vector $B$ with a fixed magnetic field strength $H$ can be plotted in 3-D space. These parameters can be fitted by the series magnetization curves in Fig. 7 based on magnetic measurement results with the biased static magnetic field.

Besides, the magnetic permeability in the laminated direction of the silicon steel sheet is equivalent to the insulating air gap of the steel sheet by a homogenization method calculated by

$$\mu_z = \frac{\mu_r}{(1-F)\mu_r + F} \tag{5}$$

where $\mu_r$ is the relative permeability in the laminated direction neglecting air gap effect, $\mu_z$ is the averaged relative permeability of the bulk specimen in the laminated direction considering the air gap, and $F$ is the stacking factor of the laminated silicon steel which is measured as 0.98.

Fig. 8 depicts the contour of the magnetic energy defined by (3) of high GO silicon steel under ac and dc hybrid magnetization model.

It also shows that the magnetic properties in two directions are strongly coupled, while the traditional model in (4) neglects magnetic coupling effects which would cause the numerical errors of the 3-D laminated simulation. The range in $z$-axis of the contour is less than 0.15 T which is large enough to cover the leakage magnetic flux density along the laminated direction for electrical machine and power transformer. Furthermore, the contour of energy represents that magnetization ability in the rolling direction of silicon steel is stronger. The silicon steel shows magnetic anisotropy in $xoz$ and $yoz$ planes, and the permeability $\mu_x$ and $\mu_y$, which are dependent on the static magnetic field in the stacking direction, can be calculated from the contours in Fig. 8 for finite-element analysis.

## V. Conclusion

In this paper, the 3-D magnetic testing system is improved to measure the silicon steel sheet specimen under ac and dc hybrid excitation model. The magnetic anisotropy properties in the rolling and the transverse direction under dc-bias magnetic field along the laminated direction can be measured and expressed by the ellipsoid model. The static magnetic field applied in the stacking direction will make the magnetization process in sheet plane more difficult and increase core losses.

## Acknowledgment

This work was supported in part by the National Natural Science Foundation of China under Grant 51777055 and Grant 51807048, in part by the National Key R&D Program of China under Grant 2017YFB0903904, in part by the Hebei Province Science Foundation under Grant E2018202284 and Grant E2018202301, in part by the Scientific Research Project of Hebei University under Grant QN2018157, and in part by the Natural Science Foundation of Tianjin under Grant 15JCYBJC16400.

## References

[1] Z. Cheng *et al.*, "Analysis and measurements of iron loss and flux inside silicon steel laminations," *IEEE Trans. Magn.*, vol. 45, no. 3, pp. 1222–1225, Mar. 2009.

[2] Y. Guo, J. G. Zhu, J. Zhong, H. Lu, and J. X. Jin, "Measurement and modeling of rotational core losses of soft magnetic materials used in electrical machines: A review," *IEEE Trans. Magn.*, vol. 44, no. 2, pp. 279–291, Feb. 2008.

[3] *Standard Test Method for Alternating-Current Magnetic Properties of Materials at Power Frequencies Using Wattmeter-Ammeter-Voltmeter Method and 25-cm Epstein Test Frame*, ASTM Standard A343/A343M, Annual Book of ASTM Standards, 2003.

[4] J. Sievert, "Recent advances in the one- and two-dimensional magnetic measurement technique for electrical sheet steel," *IEEE Trans. Magn.*, vol. 26, no. 5, pp. 2553–2558, Sep. 1990.

[5] N. Stranges and R. D. Findlay, "Importance of rotational iron loss data for accurate prediction of rotating machine core losses," in *Proc. IEEE Ind. Appl. Soc. Annu. Meeting*, Oct. 1994, pp. 123–127.

[6] A. J. Moses, "Importance of rotational losses in rotating machines and transformers," *J. Mater. Eng. Perform.*, vol. 1, no. 2, pp. 235–244, Mar. 1992.

[7] Q. Yang, Y. Li, Z. Zhao, L. Zhu, Y. Luo, and J. Zhu, "Design of a 3-D rotational magnetic properties measurement structure for soft magnetic materials," *IEEE Trans. Appl. Supercond.*, vol. 24, no. 3, Jun. 2014, Art. no. 8200804.

[8] Z. W. Lin and J. G. Zhu, "Three-dimensional magnetic properties of soft magnetic composite materials," *J. Magn. Magn. Mater.*, vol. 312, pp. 158–163, May 2007.

[9] S. Zurek, P. Marketos, T. Meydan, and A. J. Moses, "Use of novel adaptive digital feedback for magnetic measurements under controlled magnetizing conditions," *IEEE Trans. Magn.*, vol. 41, no. 11, pp. 4242–4249, Nov. 2005.